Journal of Chromatography A, 1217 (2010) 6241–6249

Contents lists available at ScienceDirect

Journal of Chromatography A

journal homepage: www.elsevier.com/locate/chroma

Thermodynamic and kinetic characterization of a bridged-ethylene hybrid C_{18} stationary phase

Amber M. Hupp[1], Victoria L. McGuffin*

Department of Chemistry, Michigan State University, East Lansing, MI 48824-1322 USA

ARTICLE INFO

Article history:
Received 17 May 2010
Received in revised form 2 August 2010
Accepted 6 August 2010
Available online 13 August 2010

Keywords:
Thermodynamics
Kinetics
Reversed-phase liquid chromatography
Hybrid stationary phase
Polycyclic aromatic hydrocarbons

ABSTRACT

In this study, a series of polycyclic aromatic hydrocarbons (PAHs) and nitrogen-containing polycyclic aromatic hydrocarbons (NPAHs) is separated on a hybrid stationary phase using methanol and acetonitrile mobile phases. Temperature is varied from 283 to 313 K in order to determine thermodynamic and kinetic parameters of the separation. Thermodynamic behavior is characterized by the retention factor and associated changes in molar enthalpy, whereas kinetic behavior is characterized by the rate constants and associated activation energies. In this study, the retention factors for the NPAHs are smaller than those for the parent PAHs in methanol, while they are more similar to the parent PAHs in acetonitrile. The changes in molar enthalpy are very similar for all solutes, yet are more negative in acetonitrile than in methanol. The rate constants for the NPAHs are smaller than those for their parent PAHs in both mobile phases. Moreover, the rate constants in acetonitrile are one to four orders of magnitude smaller than those in methanol. Based on these thermodynamic and kinetic results, the hybrid stationary phase is compared to traditional silica stationary phases. In addition, the relative contributions from the partition and adsorption mechanisms are discussed.

1. Introduction

Silica-based supports remain the most widely used materials for reversed-phase liquid chromatography (RPLC) separations. Many improvements have been made in recent years that address chromatographic problems related to the silica support. For example, high-purity silica has reduced peak tailing from metallic impurities [1,2], while trifunctional and sterically hindered monofunctional silanes influence interaction of solutes with the underlying support [3,4]. Similarly, phases incorporating a polar embedded group have been used to shield the underlying support in an effort to reduce peak tailing while modifying the selectivity of the separation [5–7].

The improvements made on silica supports have significantly influenced the types of separations that can currently be performed. Nevertheless, problems with silica-based materials continue to exist at high and low pH, extreme temperature, and for basic solutes that can interact with residual silanol groups in the underlying support. For this reason, a support material based on a hybrid organic–inorganic particle has been developed and widely used as an RPLC stationary phase. This bridged-ethylene hybrid (BEH) particle is synthesized by the co-condensation of 1,2-bis(triethoxysilyl)ethane with tetraethoxysilane [8]. This support particle has the mechanical strength of silica, combined with the pH [8–10] and temperature [10] stability of polymeric particles. In addition, the ethylene bridge in the backbone is thought to decrease the number of silanols available to bind to basic solutes.

The hybrid phase has been employed in many studies under a wide variety of experimental conditions. However, only a few such studies have reported thermodynamic information about the hybrid material [11,12], whereas no studies have reported kinetic information. A thermodynamic evaluation of a C_{18} hybrid phase was performed as a function of temperature (150 to 200 °C) in an aqueous mobile phase using alkyl benzenes and aromatic alcohols [11] and substituted anilines [12] as model solutes. Linear van't Hoff plots were obtained and negative changes in molar enthalpy were reported. Further investigation of toluene at a wider temperature range (30 to 200 °C) was performed. A change in slope of the van't Hoff plot near 97 °C was seen and was attributed to a change in the conformation of the stationary phase in the presence of the mobile phase [11]. Nevertheless, a direct comparison to silica-based materials was not performed and has not been reported in the literature.

Nitrogen-containing polycyclic aromatic hydrocarbons (NPAHs) are an interesting group of basic compounds that have been thoroughly investigated on silica-based materials [13,14]. NPAHs have been identified as carcinogens [15] and are commonly found in tobacco smoke [16,17], automobile exhaust [18], fossil fuels [19,20], and even lake sediment [21]. RPLC has proven useful for the separation of complex NPAHs. Their dramatic peak shapes make them

* Corresponding author. Tel.: +517 355 9715; fax: +517 353 1793.
E-mail address: jgshabus@aol.com (V.L. McGuffin).
[1] Current address: Department of Chemistry, College of the Holy Cross, One College Street, Worcester, MA 01610 USA.

0021-9673/$ – see front matter © 2010 Elsevier B.V. All rights reserved.
doi:10.1016/j.chroma.2010.08.015

a suitable set of solutes for examination of the thermodynamic and kinetic behavior of hybrid stationary phases.

In this research, a series of NPAHs and their parent polycyclic aromatic hydrocarbons (PAHs) are separated on a RPLC system using a C_{18} hybrid packing material. Thermodynamic and kinetic information is examined as function of temperature. The effect of mobile phase is examined using methanol as a model of protic solvents and acetonitrile as a model of aprotic solvents. Thermodynamic behavior is characterized by the retention factor and associated changes in molar enthalpy, whereas kinetic behavior is characterized by the rate constants and associated activation energies. This evaluation provides insight into the retention mechanism of PAHs and NPAHs on hybrid stationary phases in RPLC.

2. Theory

The determination of thermodynamic and kinetic contributions to retention requires a synthesis of traditional thermodynamic and transition state theories [22,23]. In this evaluation, the transfer between mobile and stationary phases is regarded as a chemical reaction. These theories will be discussed in the following sections.

2.1. Thermodynamics

The thermodynamic parameters describe the path-independent measures of solute transfer from the mobile to stationary phase. These parameters are calculated from the retention factor (k)

$$k = \frac{t_r - t_0}{t_0} \tag{1}$$

where t_r and t_0 are the elution times of a retained and a non-retained solute, respectively. The retention factor is related to the changes in molar enthalpy (ΔH) and molar entropy (ΔS) by the van't Hoff equation

$$\ln k = \frac{-\Delta H}{RT} + \frac{\Delta S}{R} - \ln \beta \tag{2}$$

where R is the gas constant, T is the absolute temperature, and β is the phase ratio. The change in molar enthalpy is determined from the slope of a graph of the natural logarithm of the retention factor versus the inverse temperature at constant pressure. The change in molar entropy is contained in the intercept, but cannot be reliably quantitated since the phase ratio is a function of both temperature and pressure.

2.2. Kinetics

The kinetic parameters describe the path-dependent measures of solute transfer from the mobile to stationary phase. During the transfer, the solute passes through a high-energy transition state ($\ddagger$) that uniquely characterize the path-dependent aspects of the retention mechanism. The method of calculating kinetic rate constants is derived by extrapolation of Giddings work [24]. The mass transfer term (C_s) for slow kinetics is given by

$$C_s = \frac{2k}{(1+k)^2 k_{ms}} \tag{3}$$

$$\text{Thus, } k_{ms} = \frac{2ku}{(1+k)^2 H_{corr}} \text{ and } k_{sm} = \frac{2k^2 u}{(1+k)^2 H_{corr}} \tag{4}$$

where k_{ms} is the rate constant for transfer from stationary to mobile phase, k_{sm} is the rate constant for transfer from mobile to stationary phase, and u is the linear velocity. The corrected plate height (H_{corr}) represents slow mass transfer in the stationary phase (C_s), and is calculated by

$$H_{corr} = C_s u = H - A - \frac{B_m}{u} - \frac{B_s}{u} - C_m u \tag{5}$$

where A, B_m, B_s, and C_m are the classical contributions to zone broadening arising from multiple paths, diffusion in the mobile and stationary phases, and resistance to mass transfer in the mobile phase, respectively [24]. The kinetic rate constants can be expressed by means of the Arrhenius equation

$$\ln k_{sm} = \ln A_{\ddagger m} - \frac{\Delta E_{\ddagger m}}{RT} \tag{6}$$

$$\ln k_{ms} = \ln A_{\ddagger s} - \frac{\Delta E_{\ddagger s}}{RT} \tag{7}$$

where $A_{\ddagger m}$ and $A_{\ddagger s}$ are the pre-exponential factors. The activation energies ($\Delta E_{\ddagger m}$ and $\Delta E_{\ddagger s}$) are determined from the slope of a graph of the natural logarithm of the rate constants (k_{sm} and k_{ms}) versus inverse temperature at constant pressure.

3. Experimental methods

3.1. Reagents

As shown in Fig. 1, two polycyclic aromatic hydrocarbons (PAHs) and six nitrogen-containing PAHs (NPAHs) are chosen to study the effect of nitrogen position, ring number, and annelation structure on the thermodynamics and kinetics of retention. Pyrene, benz[a]anthracene, 1-aminopyrene (Sigma-Aldrich), 1-azapyrene, 4-azapyrene, benz[a]acridine, dibenz[c,h]acridine, and dibenz[a,j]acridine (Institute für PAH Forschung) are obtained as solids and dissolved in high-purity methanol and acetonitrile (Burdick and Jackson Division, Honeywell) to yield standard solutions with concentrations between 10^{-3} M and 10^{-5} M. The concentration of each solute is chosen to be well below the solubility limit in both methanol and acetonitrile. A non-retained marker, 4-bromomethyl-7-methoxycoumarin (Sigma), is added to each solution at a concentration of 10^{-3} M.

3.2. Instrumental system

The solutes are separated via a capillary liquid chromatography system that has been described previously [22]. A fused-silica capillary (200 μm i.d., 89 cm length, Polymicro Technologies) is packed by the slurry method and terminated with a quartz wool frit. Columns prepared in this manner have uniform packing across the column diameter and along the column length [25]. The packing material (XBridge C_{18}, Waters Corporation) is prepared by reaction of surface silanols on the bridged-ethylene hybrid support with octadecyltrichlorosilane at a bonding density of 3.06 μmol/m^2 [8]. Unreacted surface silanols are end-capped with trimethylchlorosilane [8]. The resulting stationary phase is characterized by a 5.2 μm particle size, 141 Å pore size, and 189 m^2/g surface area.

The methanol and acetonitrile mobile phases are delivered via a single-piston reciprocating pump (Model 114 M, Beckman Instruments) that is operated in constant-pressure mode at 2000 psi. The sample is introduced by a 1.0 μL injection valve (Model ECI4W1, Valco Instruments), where the injection volume is split between the capillary column and a fused-silica capillary (50 μm i.d., Polymicro Technologies), resulting in an injection volume of 10 nL. A fused-silica capillary (20 μm i.d., Polymicro Technologies) is attached post-column to serve as a restrictor. The injector, column, splitter, and restrictor are enclosed within a cryogenic oven (Model 3300, Varian Associates) that enables the temperature to be varied from 283 to 313 K (± 0.1 K).

Solute detection is achieved by on-column laser-induced fluorescence. A continuous-wave helium-cadmium laser (Model

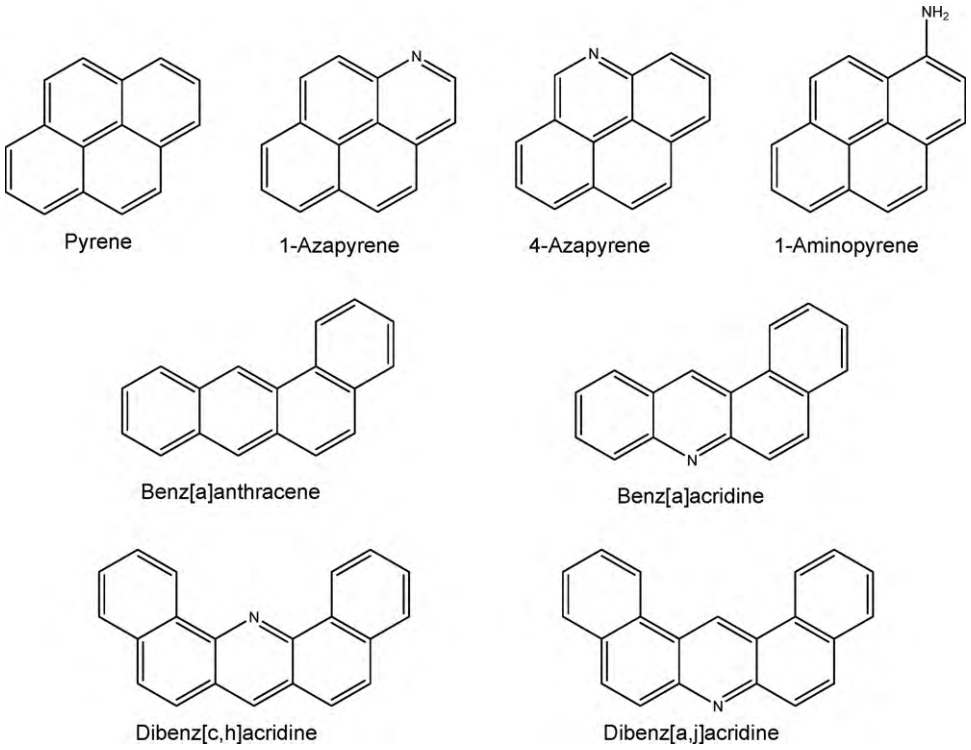

Fig. 1. Structure of the polycyclic aromatic hydrocarbons (PAHs) and nitrogen-containing polycyclic aromatic hydrocarbons (NPAHs).

3074-20 M, Melles Griot), with approximately 34 mW power at 325 nm, is used as the excitation source. The laser is focused onto UV-grade optical fibers (100 μm, Polymicro Technologies) and is transmitted to two locations along the column (39.2 and 74.7 cm), where the polyimide coating of the capillary has been removed. The fluorescence power at each location is collected orthogonally by large diameter optical fibers (500 μm, Polymicro Technologies), isolated by a 420-nm interference filter (S10-410-F, Corion), and transmitted to a photomultiplier tube (Model R760, Hamamatsu). The resulting photocurrent is amplified, converted to the digital domain (PCI-MIO-16XE-50, National Instruments), and stored by a user-defined program (Labview v5.1, National Instruments).

3.3. Data analysis

To extract thermodynamic and kinetic information, statistical moments are used because they make no assumptions about the shape of the solute zone profiles or the mechanism of retention. The individual zone profiles are extracted from the chromatogram and are fit by using nonlinear regression (Tablecurve v4.14, SYSTAT Software, Inc.), so that the statistical moments can be determined without contributions from noise. A combination of Gaussian and asymmetric double sigmoidal [26] equations produces excellent fit, with random residuals and correlation coefficients ranging from 0.999 to 0.956. The zone profile is then regenerated in a spreadsheet program (Excel v2003, Microsoft Corp.). In this work, the peak boundaries are identified at 0.1% of the maximum peak height, as the error in the calculation of the statistical moments is small at this integration limit [27]. Statistical moments are calculated based on the regenerated profile by

$$M_1 = \frac{\int C(t)\, t\, dt}{\int C(t) dt} \tag{8}$$

$$M_2 = \frac{\int C(t)(t - M_1)^2 dt}{\int C(t) dt} \tag{9}$$

$$M_3 = \frac{\int C(t)(t - M_1)^3 dt}{\int C(t) dt} \tag{10}$$

where C(t) is the solute concentration as a function of time, and M_1, M_2, and M_3 are the mean retention time, variance, and asymmetry, respectively. Detection at two points along the chromatographic column allows the retention factor (k) and plate height (H) to be calculated by difference. Thus, they are calculated from the moments as

$$k = \frac{(\Delta M_1 - \Delta t_0)}{\Delta t_0} \tag{11}$$

$$H = \frac{\Delta M_2 \Delta L}{(\Delta M_1)^2} \tag{12}$$

where Δt_0 is the difference in the elution time of a non-retained species, ΔM_1 is the difference in the first moment, ΔM_2 is the difference in the second moment, and ΔL is the distance between two on-column detectors. The difference method eliminates extra-column contributions, both symmetric and asymmetric, and has been thoroughly evaluated by Hupp and McGuffin [28]. The corrected plate height is then calculated using Equation 5 [28], where the sum of the A, B_m, B_s, and C_m terms is equal to 0.001 cm for pyrene and benz[a]anthracene. It is noteworthy that this value is approximately two times the particle diameter (5 μm).

In addition, the statistical moments can be used to calculate the skew (S) as

$$S = \frac{M_3}{M_2^{3/2}} \tag{13}$$

The skew describes the asymmetry, where a positive value indicates a tailing peak and a negative value indicates a fronting peak. A larger value for the skew indicates a more asymmetric peak.

4. Results and discussion

The mobile phase has been shown to influence strongly the separation of PAHs and NPAHs on silica-based stationary phases [13]. For this reason, a similar study is warranted for the bridged-ethylene hybrid stationary phases. In this study, both protic (methanol) and aprotic (acetonitrile) solvents are evaluated. Many studies have investigated the properties of these organic solvents [29,30], and selected parameters for polarity, acidity, and basicity are summarized in the Supplementary Information. Overall, methanol is more polar than acetonitrile, however the contributions to this polarity differ significantly. Methanol has greater hydrogen bonding interactions, while acetonitrile has greater polarizability and dipole moment. Among the hydrogen bonding interactions (both Bronsted and Lewis types), methanol is stronger as a base and substantially stronger as an acid than acetonitrile. Even more important, however, is how these solvent properties influence the acid/base character of other species. For example, the dissociation constants of weak acids (K_a) are typically 10–15 orders of magnitude stronger in methanol than in acetonitrile. The dissociation constants of weak bases (K_b) are typically 9–11 orders of magnitude stronger in methanol than in acetonitrile. Thus, the methanol mobile phase can form hydrogen bonds with the NPAH solutes, inhibiting their ability to adsorb at silanol sites. Methanol can also form hydrogen bonds with residual silanol sites in the hybrid support, displacing or competing with the NPAHs. In these ways, methanol reduces the interactions of the NPAHs with silanol sites. However, acetonitrile cannot undergo hydrogen bonding with NPAHs and silanol groups to the same extent and, therefore, cannot inhibit their interaction. Consequently, a comparison of retention behavior in these solvents is of interest on the bridged-ethylene hybrid stationary phases. Pure methanol and acetonitrile have been used as mobile phases, rather than aqueous–organic mixtures, because the solvent properties of water tend to predominate even at low concentrations (see Supplementary Information). In addition, this assures that the solvent composition is uniform in the bulk mobile phase, at the stationary phase interface, and in the pores, thereby avoiding the formation of "microphases" [31,32].

4.1. Methanol mobile phase

A representative series of chromatograms in shown in Fig. 2. In methanol, a neutral solute, such as pyrene (Fig. 2A), has a symmetric peak shape (S = 0.36, Equation 13). However, a basic solute, such as 4-azapyrene (Fig. 2B), has a tailing peak shape (S = 2.47). The peak shape for pyrene is representative of benz[a]anthracene, 1-aminopyrene, and dibenz[c,h]acridine. The peak shape for 4-azapyrene is representative of the remaining NPAHs.

4.1.1. Thermodynamic behavior

4.1.1.1. Retention factor. Retention factors for the PAHs and NPAHs are summarized in Table 1. For the most part, retention factors for the NPAHs are notably smaller than those for the parent PAHs. The retention factors for 1-aminopyrene and 4-azapyrene are smaller by 76% and 20% than pyrene, respectively. In addition, the retention factor for benz[a]acridine is smaller by 45% than benz[a]anthracene. This decreased retention behavior is due to the increased polarity of the NPAHs relative to the PAHs and is consistent with a partition mechanism. This behavior was also observed with stationary phases built on silica supports [13]. In addition, retention increases with the number of aromatic rings and with less condensed annelation structure. These trends are consistent with a partition mechanism and were also observed with phases built on silica supports [13]. The predominance of the partition mechanism for nonpolar solutes on alkylsilica phases has been demonstrated previously by Ranatunga and Carr [32].

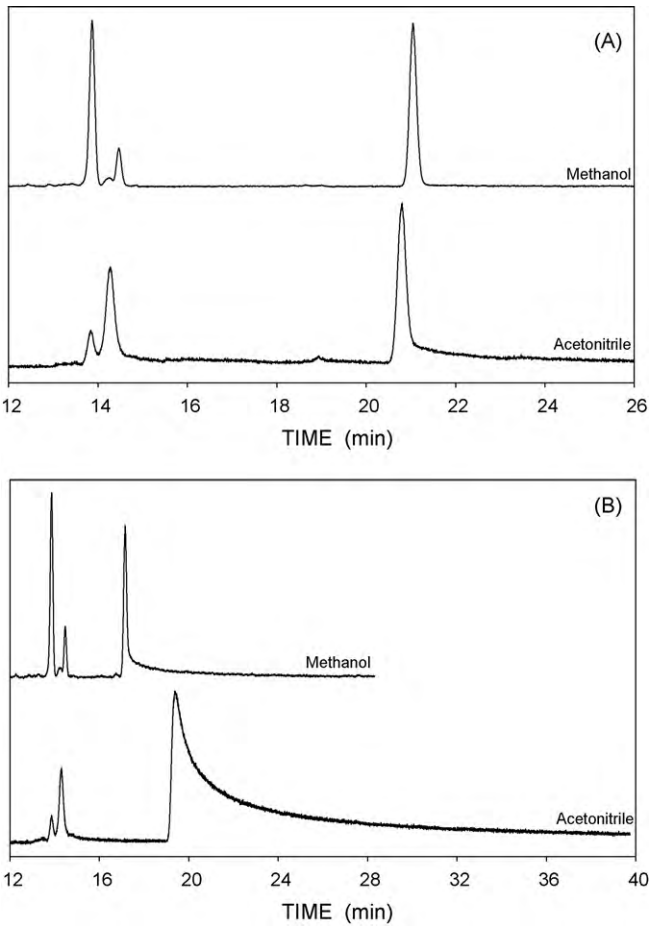

Fig. 2. Representative chromatograms of (A) pyrene and (B) 4-azapyrene in methanol and acetonitrile mobile phases at 303 K.

The effect of temperature is demonstrated in Table 1. Retention factors decrease significantly (13–45%) with increasing temperature, with the exception of the azapyrenes. 1-Azapyrene and 4-azapyrene fluctuate, yet increase (32%) or remain relatively constant with temperature, respectively. A decrease in retention factor with temperature is expected under a partition-dominated mechanism.

4.1.1.2. Molar enthalpy. A representative semi-logarithmic graph of the retention factor versus inverse temperature (van't Hoff plot) is shown in Fig. 3. The graph for each solute in Fig. 3A is linear (R^2 = 0.973–0.997) and the slope is positive. A linear graph indicates

Table 1
Retention factor (k) and change in molar enthalpy (ΔH) for PAH and NPAH solutes in methanol at 2000 psi. Values in parentheses have large errors and are given for illustrative purposes only. See text for more detail. Solutes: pyrene (P), 1-aminopyrene (1AmP), 1-azapyrene (1AzaP), 4-azapyrene (4AzaP), benz[a]anthracene (B[a]A), benz[a]acridine (B[a]Ac), dibenz[a,j]acridine (D[aj]Ac), dibenz[c,h]acridine (D[ch]Ac).

Solute	k		ΔH (kcal/mol)
	288 K	313 K	
P	0.78	0.55	-2.5 ± 0.1
1AmP	0.15	0.13	-1.4 ± 0.1
1AzaP	0.62	0.82	(3.1 ± 1.4)
4AzaP	0.45	0.44	(1.6 ± 1.1)
B[a]A	0.92	0.62	-3.0 ± 0.1
B[a]Ac	0.43	0.34	-1.6 ± 0.1
D[aj]Ac	0.92	0.51	-4.0 ± 0.3
D[ch]Ac	1.80	1.02	-4.3 ± 0.2

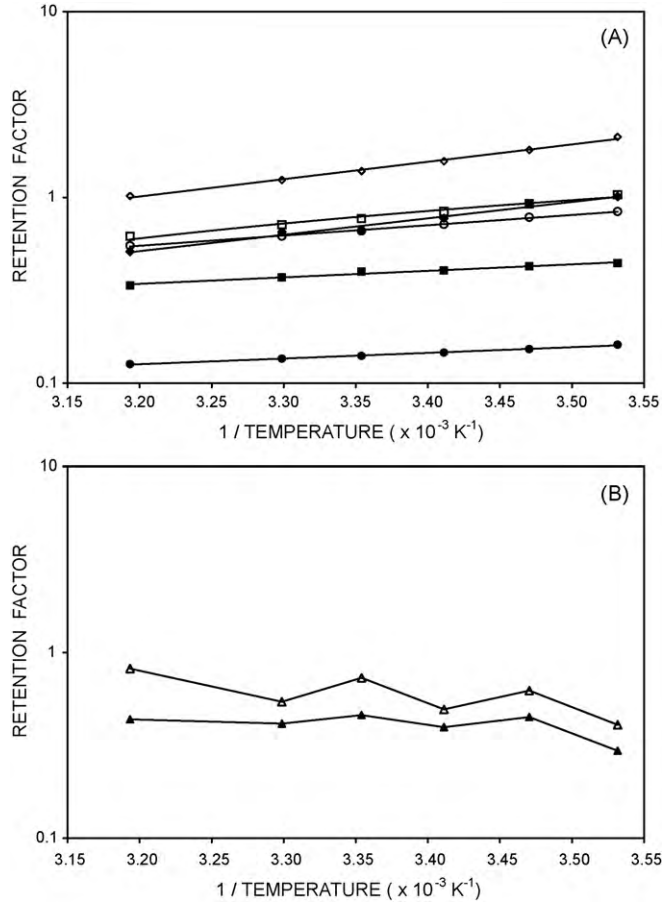

Fig. 3. Representative semi-logarithmic graph of the retention factor versus inverse temperature for methanol mobile phase (Equation 2). (A): pyrene (○), 1-aminopyrene (●), benz[a]anthracene (□), benz[a]acridine (■), dibenz[a,j]acridine (♦), dibenz[c,h]acridine (◊). (B): 1-azapyrene (△), 4-azapyrene (▲).

that the change in molar enthalpy is constant over the temperature range of the study (283–313 K), which suggests that there is no significant change in retention mechanism in this region. A positive slope indicates a negative change in molar enthalpy, suggesting the transfer from mobile to stationary phase is an enthalpically favorable process. The graph of 1-azapyrene and 4-azapyrene in Fig. 3B is roughly linear (R^2 = 0.554 and 0.346), however the slope is negative. A negative slope indicates a positive change in molar enthalpy, suggesting the transfer from mobile to stationary phase is not enthalpically favorable.

The change in molar enthalpy is calculated for each solute from the slope of this graph, according to Equation 2, and is summarized in Table 1. The changes in molar enthalpy are least negative (least favorable) for 1-aminopyrene and benz[a]acridine, followed by pyrene and benz[a]anthracene, and most negative (most favorable) for dibenz[a,j]acridine and dibenz[c,h]acridine. These trends indicate that the change in molar enthalpy becomes more negative with increasing ring number and with less condensed annelation structure for both neutral PAHs and basic NPAHs. These trends were also observed on silica-based stationary phases and have been discussed in detail previously [13,33]. The change in molar enthalpy may be attributed to the depth to which each PAH can penetrate into the stationary phase. The proximal regions, where the alkyl group is bound to the silica surface, are highly ordered with all trans carbon–carbon bonds. As the distance from the surface increases, there are more gauche bonds and greater disorder [34–36]. The more condensed PAHs, such as pyrene, probe only the distal regions of the alkyl chain, while less condensed PAHs, such as benz[a]anthracene, penetrate more deeply into the ordered regions of the alkyl chain. Therefore, the change in molar enthalpy becomes more negative as the PAH can access the inner regions of the stationary phase.

Table 2
Rate constants for transfer from mobile to stationary phase (k_{sm}) and from stationary to mobile phase (k_{ms}) for PAH and NPAH solutes in methanol at 2000 psi. Solutes defined in Table 1.

Solute	k_{sm} (s^{-1})		k_{ms} (s^{-1})	
	288 K	313 K	288 K	313 K
P	0.53	120	0.69	220
1AmP	4.1	–[a]	27	–
1AzaP	0.003	0.003	0.005	0.003
4AzaP	0.006	0.006	0.009	0.01
B[a]A	460	–	500	–
B[a]Ac	0.02	0.03	0.03	0.09
D[aj]Ac	0.04	0.49	0.03	0.96
D[ch]Ac	15	180	8.1	500

[a] Values not accurately determined, see discussion in text.

The change in molar enthalpy is positive for 1-azapyrene and 4-azapyrene, corresponding to the negative slope in the van't Hoff plot. However, the slopes of these lines are associated with large errors. Despite the uncertainty in the measurement, some discussion of this interesting behavior is warranted. At high temperature, the alkyl chains of the stationary phase become more fluid-like and flexible, making the surface of the underlying particle more accessible. It is possible that at the higher temperatures used in this study, 1- and 4-azapyrene are able to access the underlying particle more easily. In this case, these solutes may be able to adsorb more strongly at the residual silanol sites. Thus, the retention mechanism for these solutes may change over the temperature range investigated. The change in molar enthalpy is not meaningful when two separate processes, in this case partition and adsorption mechanisms, are occurring. It is noteworthy that the other 4-ring NPAH, benz[a]acridine, does not display the same behavior. Because of the condensed annelation structure and the position of the nitrogen atom (see Fig. 1), 1-azapyrene has the smallest cross-section (~2 fused aromatic rings) that must be transported toward the particle surface in the adsorption mechanism. 4-Azapyrene is only slightly larger (~2.5 fused rings), whereas benz[a]acridine is significantly larger (~3.5 fused rings). For this reason, benz[a]acridine and the larger NPAHs are still retained predominantly by the partition mechanism and do not display the anomalous thermodynamic behavior observed for the azapyrenes.

4.1.2. Kinetic behavior

Thermodynamics provides information about steady-state behavior for the change between mobile and stationary phases, however it does not fully explain the retention mechanism. The pseudo-first order rate constants and activation energies (Equations 4, 6, and 7) help to quantify the kinetic aspects of mass transfer between the mobile and stationary phases as a function of solute structure. These data provide more detailed and specific information about the retention mechanism that is not available from thermodynamic data alone.

4.1.2.1. Rate constants. Rate constants for the PAHs and NPAHs are summarized in Table 2. In methanol, benz[a]anthracene, 1-aminopyrene, and dibenz[c,h]acridine undergo the fastest rate of mass transfer, followed by pyrene, benz[a]acridine, and dibenz[a,j]acridine, with 1-azapyrene and 4-azapyrene having the slowest rate of transfer. The values for 1-azapyrene and 4-azapyrene are given only as an indication of their slow rate of transfer; the kinetic rate constants are not reliable based on the uncertainty in the experimental measurements for those

solutes, as discussed in Section 4.1.1. The rate-limiting step for dibenz[c,h]acridine is the transfer from stationary to mobile phase, since the retention factor ($k = k_{sm}/k_{ms}$) is greater than unity. In contrast, the rate-limiting step for all other solutes is the transfer from mobile to stationary phase, since the retention factor is less than unity.

The rate constants for the four-ring NPAHs are notably smaller than those for their parent PAHs, with the exception of 1-aminopyrene. 1-Azapyrene and 4-azapyrene have rate constants that are two orders of magnitude smaller than pyrene. The rate constant for benz[a]acridine is one order of magnitude larger than that for the azapyrenes, but many orders of magnitude smaller than that for benz[a]anthracene. In these cases, the nitrogen in the azapyrenes and benz[a]acridine can adsorb to silanol groups, causing a decrease in the rate constant compared to the parent PAHs. This trend was observed in the thermodynamic data (Section 4.1.1.2, Table 1) for the azapyrenes, but not for benz[a]acridine. However, it is important to note that thermodynamics reflects only differences in the initial and final states (i.e., desorbed and sorbed). A small contribution from adsorption in a predominantly partition mechanism may not cause an observable difference in the molar enthalpy or entropy. In contrast, the kinetic data provide a more sensitive indication of the retention mechanism, especially if the contributing states have significantly different rate constants, as is the case here for adsorption and partition.

The effect of temperature is demonstrated in Table 2. The rate constants for most solutes increase significantly, while the rate constants for 1-azapyrene and 4-azapyrene decrease with increasing temperature. Rate constants are not provided for 1-aminopyrene and benz[a]anthracene at the highest temperature due to overcorrection of the plate height for these narrow peaks. According to Equation 5, if the sum of the theoretical A, B, and C terms is larger than the observed plate height, an overcorrection will occur that causes H_{corr} to be negative and the rate constants to be indeterminate. This is common for very narrow peaks, where the theoretical correction terms overestimate the width of the experimental zone profile [28]. The increase in rate constants with temperature observed for most solutes is expected, owing to increased diffusion coefficients and enhanced fluidity of the stationary phase. With increased temperature, the increase in kinetic energy allows the alkyl chains to become more labile, which in turn allows the solutes to diffuse in and out of the stationary phase more freely.

4.1.2.2. Activation energy. A representative semi-logarithmic graph of the rate constant versus the inverse temperature (Arrhenius plot) is shown in Fig. 4. This graph does not contain information for 1-azapyrene and 4-azapyrene, due to uncertainty in the rate constant measurements (Section 4.1.2.1), or for 1-aminopyrene, due to its narrow peak shape and the overcorrection discussed previously (Section 4.1.2.1). Of those shown, the graph for each solute is roughly linear ($R^2 = 0.442–0.980$) and the slope is negative. A negative slope is indicative of a positive energy barrier for mass transfer.

The activation energy is calculated from the slope of this graph, according to Equations 6 and 7, and is summarized in Table 3. The activation energies are positive for all solutes listed. The activation energy from stationary phase to transition state ($\Delta E_{‡s}$) is greater than that from mobile phase to transition state ($\Delta E_{‡m}$). These results indicate that it is easier for the solutes to enter the stationary phase than to exit. With the exception of benz[a]acridine, all solutes seem to have a similar activation energy, which suggests they encounter a similar barrier at the interface between mobile and stationary phases. If the activation energies are comparable to one another, then the difference in rate constant must arise from the pre-exponential term, according to Equations 6 and 7.

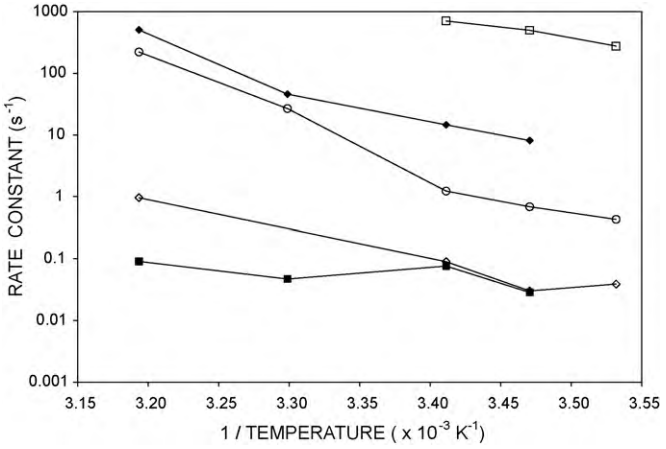

Fig. 4. Representative semi-logarithmic graph of the rate constant versus inverse temperature for methanol mobile phase (Equation 6). Pyrene (○), benz[a]anthracene (□), benz[a]acridine (■), dibenz[a,j]acridine (♦), dibenz[c,h]acridine (◊).

Table 3
Activation energies from mobile phase to transition state ($\Delta E_{‡m}$) and from stationary phase to transition state ($\Delta E_{‡s}$) for PAH and NPAH solutes in methanol at 2000 psi. Solutes defined in Table 1.

Solute	$\Delta E_{‡m}$ (kcal/mol)	$\Delta E_{‡s}$ (kcal/mol)
P	37 ± 4	39 ± 4
B[a]A	30 ± 11	33 ± 10
B[a]Ac	2 ± 3	6 ± 3
D[aj]Ac	17 ± 3	21 ± 4
D[ch]Ac	25 ± 5	29 ± 4

According to transition-state theory, the pre-exponential term is a measure of the activation entropy ($\Delta S_{‡m}$ and $\Delta S_{‡s}$) for the transfer between phases. Interestingly, the activation energies for solutes on this hybrid phase are similar to those reported on silica-based phases [13,33].

4.2. Acetonitrile mobile phase

A representative series of chromatograms is shown in Fig. 2. In acetonitrile, a neutral solute, such as pyrene (Fig. 2A), has a tailing peak shape (S = 2.68, Equation 13). However, a basic solute, such as 4-azapyrene (Fig. 2B), has a much more pronounced tailing peak shape (S = 19.0). The peak shapes for benz[a]anthracene and 1-aminopyrene remain symmetric (S = 0.0) in acetonitrile. The peak shape for pyrene is representative of dibenz[c,h]acridine. The peak shape for 4-azapyrene is representative of the remaining NPAHs.

4.2.1. Thermodynamic behavior

4.2.1.1. Retention factor. Retention factors for the PAHs and NPAHs are summarized in Table 4. When compared to the methanol mobile

Table 4
Retention factor (k) and change in molar enthalpy (ΔH) for PAH and NPAH solutes in acetonitrile at 2000 psi. Solutes defined in Table 1.

Solute	k		ΔH (kcal/mol)
	288 K	313 K	
P	0.82	0.52	-3.5 ± 0.2
1AmP	0.23	0.16	-2.7 ± 0.1
1AzaP	1.33	0.58	(-6.8 ± 3.1)
4AzaP	0.93	0.47	-4.4 ± 0.5
B[a]A	0.78	0.47	-3.7 ± 0.1
B[a]Ac	0.71	0.33	-5.9 ± 0.4
D[aj]Ac	1.56	0.76	-6.0 ± 0.5
D[ch]Ac	1.64	0.91	-4.4 ± 0.2

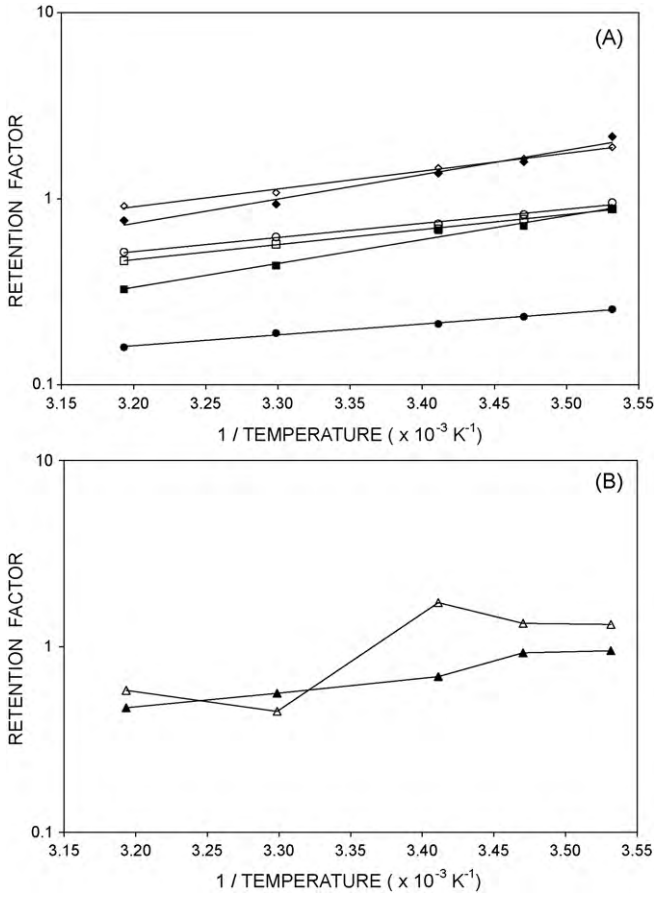

Fig. 5. Representative semi-logarithmic graph of the retention factor versus inverse temperature for acetonitrile mobile phase (Equation 2). (A): pyrene (○), 1-aminopyrene (●), benz[a]anthracene (□), benz[a]acridine (■), dibenz[a,j]acridine (♦), dibenz[c,h]acridine (◊). (B): 1-azapyrene (△), 4-azapyrene (▲).

phase (Table 1), almost all solutes demonstrate an increase in retention factor in acetonitrile. The increase is moderate for pyrene (5%), but is more substantial for the other solutes (50–69%). In contrast, benz[a]anthracene and dibenz[c,h]acridine show a decrease in retention in acetonitrile. Since acetonitrile is less polar than methanol, the retention factor would be expected to decrease if the partition mechanism were dominant. Thus, the observed increase in retention factor for many solutes suggests that the adsorption mechanism is contributing more greatly in acetonitrile than in methanol. In addition, retention factors for the NPAHs are very similar to or larger than those for the parent PAHs, which also indicates that the adsorption mechanism may be dominant for these solutes in acetonitrile.

The effect of temperature is demonstrated in Table 4. Retention factors decrease significantly with increasing temperature. In fact, for the same change in temperature, the decrease is more significant in acetonitrile than in methanol (Table 1).

4.2.1.2. Molar enthalpy. A representative semi-logarithmic graph of the retention factor versus inverse temperature (van't Hoff plot) is shown in Fig. 5. The graph for each solute in Fig. 5A is linear (R^2 = 0.978–0.999) and the slope is positive. The positive slope indicates a negative change in molar enthalpy, suggesting the transfer from mobile to stationary phase is an enthalpically favorable process for these solutes. The graph of 1-azapyrene and 4-azapyrene in Fig. 5B is roughly linear (R^2 = 0.573 and 0.929), however due to the uncertainty in the measurement, the thermodynamic and kinetic information for these solutes is unreliable and is given for illustrative purposes only.

The change in molar enthalpy is summarized for all solutes in Table 4. The change in molar enthalpy is least negative (least favorable) for 1-aminopyrene, followed by pyrene, benz[a]anthracene, and dibenz[c,h]acridine. The change in molar enthalpy is most negative (most favorable) for benz[a]acridine and dibenz[a,j]acridine. These trends indicate that the change in molar enthalpy does not consistently become more negative with increasing ring number and with less condensed annelation structure, as would be expected for a partition mechanism. The changes in molar enthalpy are more negative in acetonitrile (Table 4) than in methanol (Table 1) for most solutes by 1.0–4.3 kcal/mol. This change in molar enthalpy is consistent with an adsorption mechanism for most solutes [13]. However, the change in molar enthalpy is more comparable in acetonitrile and methanol for benz[a]anthracene and dibenz[c,h]acridine (0.1–0.7 kcal/mol). This suggests that the partition mechanism is still important for these solutes, such that the less polar mobile phase, acetonitrile, competes more effectively than methanol with the nonpolar stationary phase. These solutes are suspected to have less basic character, due to lack of nitrogen (benz[a]anthracene) and sterically-hindered nitrogen (dibenz[c,h]acridine), and hence, have less adsorption at residual silanol sites.

The differences in molar enthalpy in acetonitrile (Table 4) and methanol (Table 1) are a direct indication of the differences in retention factor. That is, the slopes of the van't Hoff plots in the two solvents are not comparable to one another. In contrast, the intercepts of the van't Hoff plots in acetonitrile and methanol are quite similar. According to the van't Hoff equation (Equation 2), the similarity in intercepts suggests that the molar entropy does not change significantly with solvent.[2] This behavior is unlike that observed previously on silica-based materials, where the molar entropy contributed significantly more than the molar enthalpy to the difference in retention factor [13,33]. It is noteworthy, however, that not all solutes behave in this way on the hybrid stationary phases. For example, benz[a]acridine has retention factors of 0.33 and 0.34 in acetonitrile and methanol, respectively, yet the change in molar enthalpy is significantly more negative in acetonitrile (-5.9 kcal/mol) than in methanol (-1.6 kcal/mol). To allow for such similar values of the retention factor, either the molar entropy or the phase ratio must change significantly according to the van't Hoff equation.

4.2.2. Kinetic behavior

4.2.2.1. Rate constants. Rate constants for the PAHs and NPAHs are summarized in Table 5. In acetonitrile, benz[a]anthracene and 1-aminopyrene undergo the fastest rate of transfer, followed by pyrene, benz[a]acridine, dibenz[a,j]acridine, and dibenz[c,h]acridine, which are three orders of magnitude slower. 1-Azapyrene and 4-azapyrene have the slowest rate of transfer, an order of magnitude slower than the majority of the solutes. 1-Azapyrene and 4-azapyrene are given only as an indication of their slow rate of transfer. As stated previously in Section 4.1.2.1, the kinetic values are not reliable based on the uncertainty in the experimental measurement for those solutes. The rate constants in acetonitrile are one to four orders of magnitude smaller than those in methanol (Table 2). The differences in the rate constants result from the increased ability of the NPAHs to interact with residual silanols on the hybrid support. The aprotic solvent, acetonitrile,

[2] Alternatively, it may suggest that any change in the molar entropy is compensated by an equal but opposite change in the phase ratio. Because any changes in the phase ratio should be similar for hybrid and silica-based materials, this alternative explanation is less plausible.

Table 5
Rate constants for transfer from mobile to stationary phase (k_{sm}) and from stationary to mobile phase (k_{ms}) for PAH and NPAH solutes in acetonitrile at 2000 psi. Solutes defined in Table 1.

Solute	k_{sm} (s^{-1})		k_{ms} (s^{-1})	
	288 K	313 K	288 K	313 K
P	0.02	0.08	0.03	0.16
1AmP	0.24	–[a]	1.1	–
1AzaP	0.002	0.003	0.002	0.005
4AzaP	0.003	0.002	0.003	0.002
B[a]A	6.2	2.1	8.4	4.7
B[a]Ac	0.02	0.003	0.03	0.02
D[aj]Ac	0.01	0.02	0.01	0.02
D[ch]Ac	0.05	0.04	0.03	0.05

[a] Values not accurately determined, see discussion in text.

does not undergo hydrogen bonding interactions with the silanol sites or solutes, as does the protic solvent, methanol. Therefore, the rate of mass transfer between the mobile and stationary phases is substantially slower.

The effect of temperature is demonstrated in Table 5. The rate constants for most solutes increase significantly, while the rate constants for 4-azapyrene, benz[a]anthracene, and benz[a]acridine decrease with increasing temperature. An increase in rate constant with temperature is expected, owing to increased diffusion coefficients and enhanced fluidity of the stationary phase.

4.2.2.2. Activation energy. A representative semi-logarithmic graph of the rate constant versus inverse temperature (Arrhenius plot) is shown in Fig. 6. The graph does not contain information for 1-azapyrene and 4-azapyrene, due to uncertainty in the rate constant measurements (Section 4.2.2.1), or for 1-aminopyrene, due to its narrow peak shape and the overcorrection discussed previously (Section 4.1.2.1). Of those shown, the graph for most solutes is roughly linear (R^2 = 0.525–0.970) and the slope is negative. A negative slope is indicative of a positive energy barrier for mass transfer. The rate constants for benz[a]anthracene fluctuate with temperature and, therefore, the slope is not linear.

The activation energy is calculated from the slope of this graph, according to Equations 6 and 7, and is summarized in Table 6. The activation energies are positive for pyrene and dibenz[a,j]acridine. The activation energy is negative for the other solutes, however, due to uncertainty in the measurements these values are not likely to be meaningful. For pyrene and dibenz[a,j]acridine, the activation energy from stationary phase to transition state ($\Delta E_{\ddagger s}$) is greater

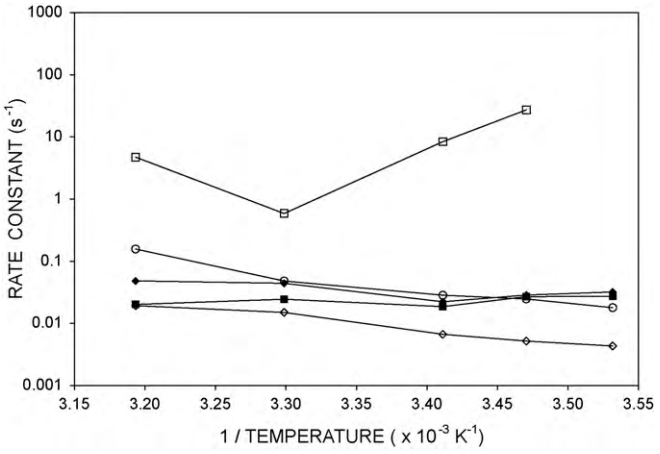

Fig. 6. Representative semi-logarithmic graph of the rate constant versus inverse temperature for acetonitrile mobile phase (Equation 6). Pyrene (○), benz[a]anthracene (□), benz[a]acridine (■), dibenz[a,j]acridine (♦), dibenz[c,h]acridine (◊).

Table 6
Activation energies from mobile phase to transition state ($\Delta E_{\ddagger m}$) and from stationary phase to transition state ($\Delta E_{\ddagger s}$) for PAH and NPAH solutes in acetonitrile at 2000 psi. Solutes defined in Table 1.

Solute	$\Delta E_{\ddagger m}$ (kcal/mol)	$\Delta E_{\ddagger s}$ (kcal/mol)
P	9 ± 2	12 ± 2
B[a]A	(-17 ± 10)	(-14 ± 10)
B[a]Ac	(-11 ± 2)	(-2 ± 1)
D[aj]Ac	4 ± 1	10 ± 1
D[ch]Ac	(-0.9 ± 2)	3 ± 2

that that from mobile phase to transition state ($\Delta E_{\ddagger m}$). These data indicate that it is easier for the solutes to enter the stationary phase than to exit. This behavior is similar to that seen in methanol.

5. Conclusions

In this study, the thermodynamic and kinetic behavior of NPAHs is examined in reversed-phase liquid chromatography using a bridged-ethylene hybrid stationary phase. The parent PAHs are separated primarily by the partition mechanism with the octadecyl groups, but some minor interaction with the residual silanol groups can occur through the π-basic aromatic system. In methanol mobile phase, the retention factors for the NPAHs are less than those for the parent PAHs. This is consistent with a partition mechanism, where retention decreases as the polarity of the solute increases. In addition, the trends of retention with ring number and annelation structure are consistent with the partition mechanism. However, the kinetic rate constants indicate that adsorption at silanol sites may play a role, as they are significantly smaller for the NPAHs than for the parent PAHs.

The different thermodynamic and kinetic behavior in the presence of the aprotic solvent acetonitrile provides an interesting and contrasting view of the retention process. Methanol is able to hydrogen bond with both the NPAH solutes and the residual silanols, which causes a reduction in the number of available silanols. Acetonitrile cannot hydrogen bond in this way to shield interactions of the solute with the underlying particle. Thus, the retention factors for the NPAHs are larger than those in methanol. Moreover, the retention factors for the NPAHs are similar to or larger than those for the PAHs, suggesting that the adsorption mechanism is likely to be dominant for the NPAH solutes. The changes in molar enthalpy are slightly more negative and are sufficient to account for the small changes in retention factor. In contrast, there does not seem to be a significant difference in the molar entropy in acetonitrile compared to methanol. The kinetic behavior also reflects the increased role of adsorption for the NPAHs, as the rate constants in acetonitrile are one to four orders of magnitude smaller than those in methanol.

The thermodynamic and kinetic behavior of the solutes on this bridged-ethylene hybrid phase is similar in nature to that on silica-based supports [13]. For the same set of solutes, the retention factors in both mobile phases are smaller on the hybrid phase than on the silica phases. The corresponding change in molar enthalpy for each solute is less negative on the hybrid phase than on the silica phases. However, it is noteworthy that the bonding density of the hybrid phase is more similar to that of the monomeric silica phase than the polymeric silica phase used in previous studies [22,37]. When this monomeric silica phase is considered, the changes in molar enthalpy are more consistent.

For the same set of solutes, the rate constants in methanol are smaller, while those in acetonitrile are comparable on the hybrid phase and on the silica phases. The corresponding activation energies in methanol are smaller, while those in acetonitrile are slightly larger for all solutes on the hybrid phase than on the silica phases. Thus, solute transfer on the hybrid phase is kinetically slower in

pure methanol, yet is more comparable in acetonitrile, when compared to the silica phases.

This thermodynamic and kinetic information provides a clear description of the retention mechanism of NPAHs on hybrid supports in reversed-phase liquid chromatography. Further studies with mobile phase additives are desirable for more thorough characterization and are currently underway.

Acknowledgements

The authors gratefully acknowledge Dr. Uwe D. Neue (Waters, Inc.) for generous donation of the hybrid stationary phase.

Appendix A. Supplementary data

Supplementary data associated with this article can be found, in the online version, at doi:10.1016/j.chroma.2010.08.015.

References

[1] J.W. Dolan, LCGC North America 23 (2005) 470.
[2] T.V. Koval'chuk, U. Lewin, V.N. Zaitsev, W. Engewald, J. Anal. Chem 54 (1999) 115.
[3] J.J. Kirkland, J.L. Glajch, R.D. Farlee, Anal. Chem 61 (1989) 2.
[4] N. Sagliano, T.R. Floyd, R.A. Hartwick, J.M. Dibussolo, N.T. Miller, J. Chromatogr. A 443 (1988) 155.
[5] J. Layne, J. Chromatogr. A 957 (2002) 149.
[6] U.D. Neue, Y.-F. Cheng, Z. Lu, B.A. Alden, P.C. Iraneta, C.H. Phoebe, K. Van Tran, Chromatographia 54 (2001) 169.
[7] J.W. Coym, J. Sep. Sci 31 (2008) 1712.
[8] K.D. Wyndham, J.E. O'Gara, T.H. Walter, K.H. Glose, N.L. Lawrence, B.A. Alden, G.S. Izzo, C.J. Hudalla, P.C. Iraneta, Anal. Chem 75 (2003) 6781.
[9] J.E. O'Gara, K.D. Wyndham, J. Liq. Chromatogr. Relat. Technol 29 (2006) 1025.
[10] T. Teutenberg, K. Hollebekkers, S. Wiese, A. Boergers, J. Sep. Sci 32 (2009) 1262.
[11] Y. Liu, N. Grinberg, K.C. Thompson, R.M. Wenslow, U.D. Neue, D. Morrison, T.H. Walter, J.E. O'Gara, K.D. Wyndham, Anal. Chim. Acta 554 (2005) 144.
[12] S. Shen, H. Lee, J. McCaffrey, N. Yee, C. Senanayake, N. Grinberg, J. Clark, J. Liq. Chromatogr. Relat. Technol 29 (2006) 2823.
[13] V.L. McGuffin, S.B. Howerton, X. Li, J. Chromatogr. A 1073 (2005) 63.
[14] H. Colin, J.-M. Schmitter, G. Guiochon, Anal. Chem 53 (1981) 625.
[15] J.C. Arcos, M.P. Argus, Chemical Introduction of Cancer, Academic Press, New York, 1974.
[16] B.L. Van Duuren, J.A. Bilbao, C.A. Joseph, J. Natl. Cancer Inst 25 (1960) 53.
[17] M. Dong, I. Schmeltz, E. Jacobs, D.J. Hoffman, J. Anal. Toxicol 2 (1978) 21.
[18] E. Sawicki, J.E. Meeker, M.J. Morgan, Arch. Environ. Health 11 (1965) 773.
[19] J.M. Schmitter, H. Colin, J.L. Excoffier, P. Arpino, G. Guiochon, Anal. Chem 54 (1982) 769.
[20] C. Borra, D. Wiesler, M. Novotny, Anal. Chem 59 (1987) 339.
[21] S.G. Wakeham, Environ. Sci. Technol 13 (1979) 1118.
[22] S.B. Howerton, V.L. McGuffin, Anal. Chem 75 (2003) 3539.
[23] V.L. McGuffin, C. Lee, J. Chromatogr. A 987 (2003) 3.
[24] J.C. Giddings, Dynamics of Chromatography, Marcel Dekker, New York, 1965.
[25] J.C. Gluckman, A. Hirose, V.L. McGuffin, M. Novotny, Chromatographia 17 (1983) 303.
[26] S.J. Gill, I. Wadso, Proc. Natl. Acad. Sci. U.S.A. 73 (1976) 2955.
[27] S.B. Howerton, C. Lee, V.L. McGuffin, Anal. Chim. Acta 478 (2003) 99.
[28] A.M. Hupp, V.L. McGuffin, J. Liq. Chromatogr. Relat. Technol. (2010), in press.
[29] C. Reichardt, Solvents and Solvent Effects in Organic Chemistry, 2nd Ed., VCH Verlagsgesellschaft, Weinheim, Germany, 1988.
[30] A.F.M. Barton, CRC Handbook of Solubility Parameters and Other Cohesion Parameters, 2nd Ed., CRC Press, Boca Raton, FL, 1991.
[31] A.M. Stalcup, D.E. Martire, S.A. Wise, J. Chromatogr. 442 (1988) 1.
[32] R.P.J. Ranatunga, P.W. Carr, Anal. Chem 72 (2000) 5679.
[33] S.B. Howerton, V.L. McGuffin, J. Chromatogr. A 1030 (2004) 3.
[34] C.J. Orendorff, M.W. Ducey Jr., J.E. Pemberton, J. Phys. Chem. A 106 (2002) 6991.
[35] M.W. Ducey Jr., C.J. Orendorff, J.E. Pemberton, L.C. Sander, Anal. Chem 74 (2002) 5576.
[36] M.W. Ducey Jr., C.J. Orendorff, J.E. Pemberton, L.C. Sander, Anal. Chem 74 (2002) 5585.
[37] V.L. McGuffin, S.-H. Chen, J. Chromatogr. A 762 (1997) 35.